Supplement of Nat. Hazards Earth Syst. Sci., 26, 1975–1996, 2026
https://doi.org/10.5194/nhess-26-1975-2026-supplement

Natural Hazards and Earth System Sciences
Open Access

Supplement of

Detection and characterization of precipitation extremes and geohydrological hazards over a transboundary Alpine area based on different methods and climate datasets

Alice Crespi et al.

Correspondence to: Alice Crespi (alice.crespi@eurac.edu)

	SPARTACUS-TST	INCA	CERRA-Land	ERA5-Land
Spatial resolution	1 km	1 km	5.5 km (0.05°)	9 km (0.1°)
Temporal resolution	daily	daily	daily	hourly
Spatial domain	Austria and South Tyrol	Greater Alpine Region	Europe	Global
Temporal coverage (at the time of the analysis)	1980-present	2003-present	1984-2021	1950 - present
Data sources	Interpolation of in situ station observations.	Integration of in situ station observations, radar data, satellite products, topographic corrections and background fields from Numerical Weather Prediction model.	Land surface model driven by meteorological forcing data from CERRA reanalysis with an offline analysis of 24-h accumulated surface precipitation integrating rain gauge data.	Land component of ERA5 reanalysis forced by meteorological fields from ERA5; no data assimilation.
Strengths	High observational accuracy; long-term temporal consistency; suitable for climate monitoring	Very high spatial and temporal resolution; strong representation of local-scale variability; good performance in complex terrain	High spatial resolution; improved representation of European topography and land-surface heterogeneity; temporally and physically consistent reconstructions of land variables	Global product widely validated and used; long temporal coverage
Limitations	Limited spatial extent; underestimation of extremes; dependent on station density	Limited spatial extent; not temporally homogeneous for climate trend analysis; methodology optimized for operational use	No direct land data assimilation; limited representation of small-scale terrain effects	Coarser resolution than regional products; limited representation of small-scale terrain effects
Main references	Hiebl and Frei, 2018; Crespi et al., 2021	Haiden et al., 2009	Ridal et al., 2024; Verelle et al., 2022	Muñoz-Sabater et al., 2021

Table S1: Key characteristics of precipitation fields of the meteorological datasets used in the study.

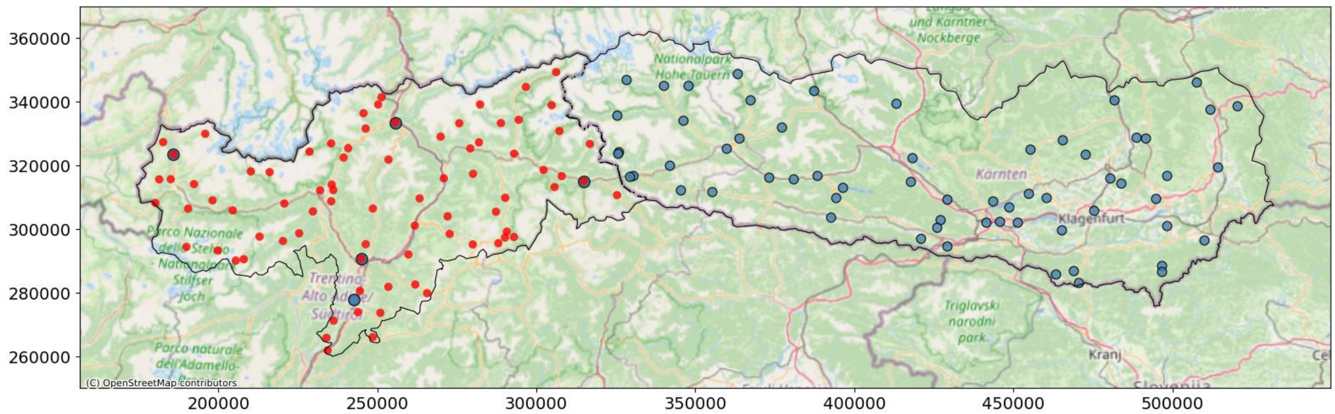

Figure S1: Map with station locations used in SPARTACUS (blue dots) and TST (red dots). Red points with blue borders are stations in common.

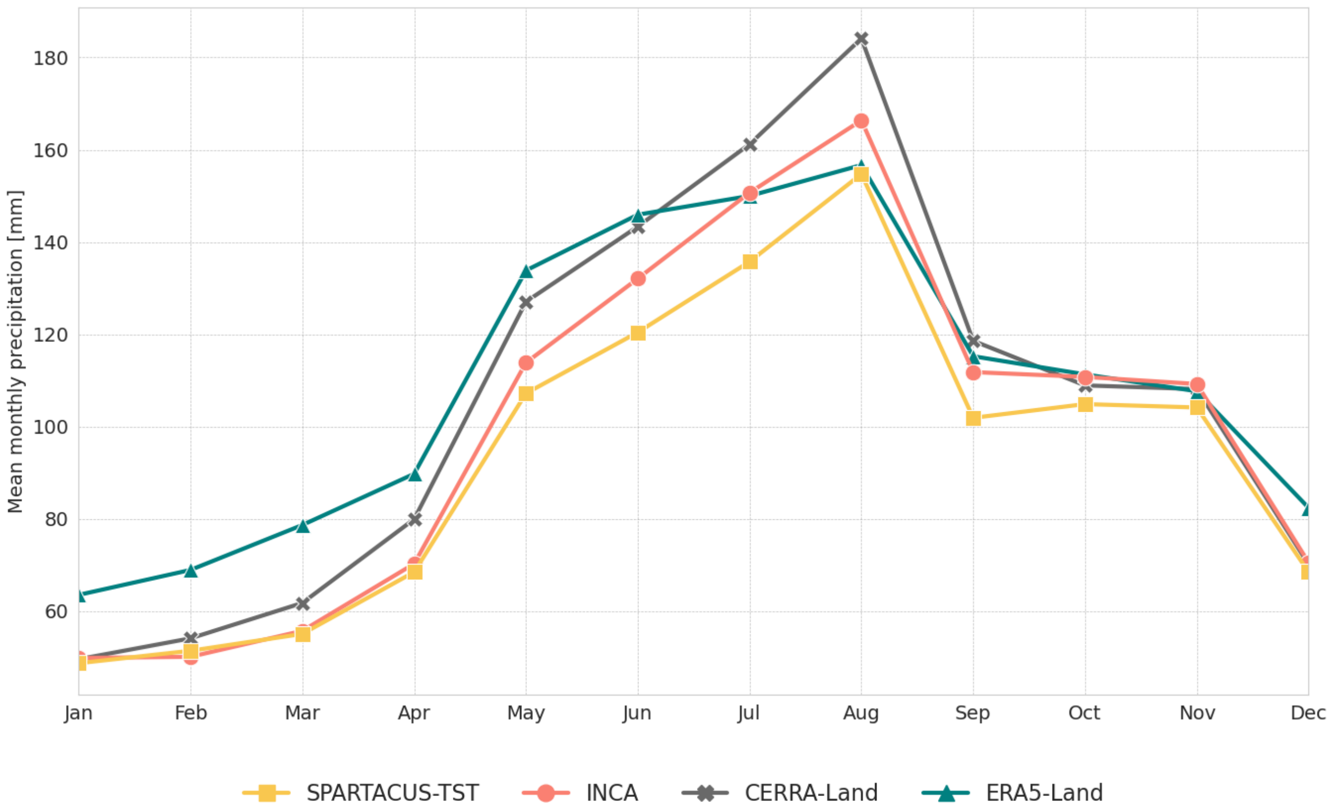

Figure S2: Mean monthly precipitation from 2003 to 2020 over the study region.

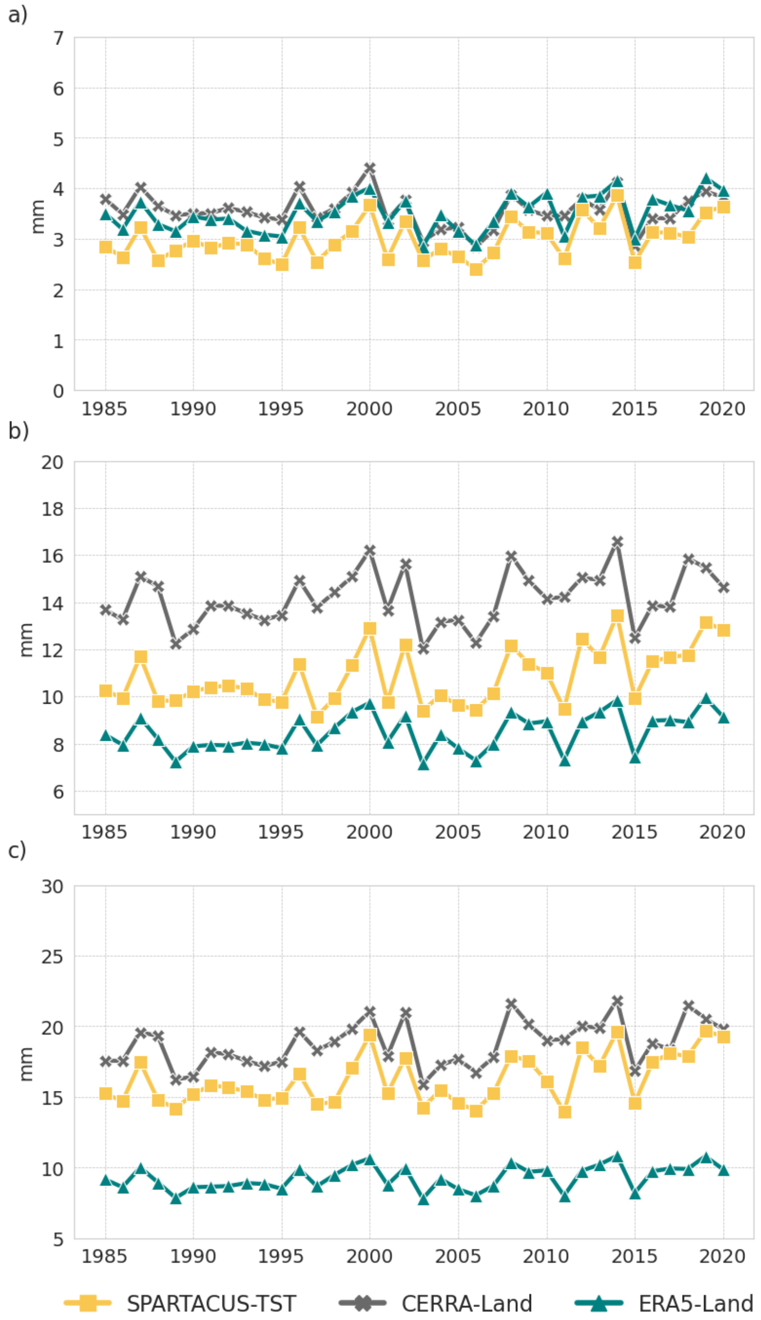

Figure S3: Annual time series 1985-2020 of the yearly averages of daily precipitation statistics: a) areal mean, b) local 99th percentile and c) local maximum over the study region based on SPARTACUS-TST, CERRA-Land and ERA5-Land.

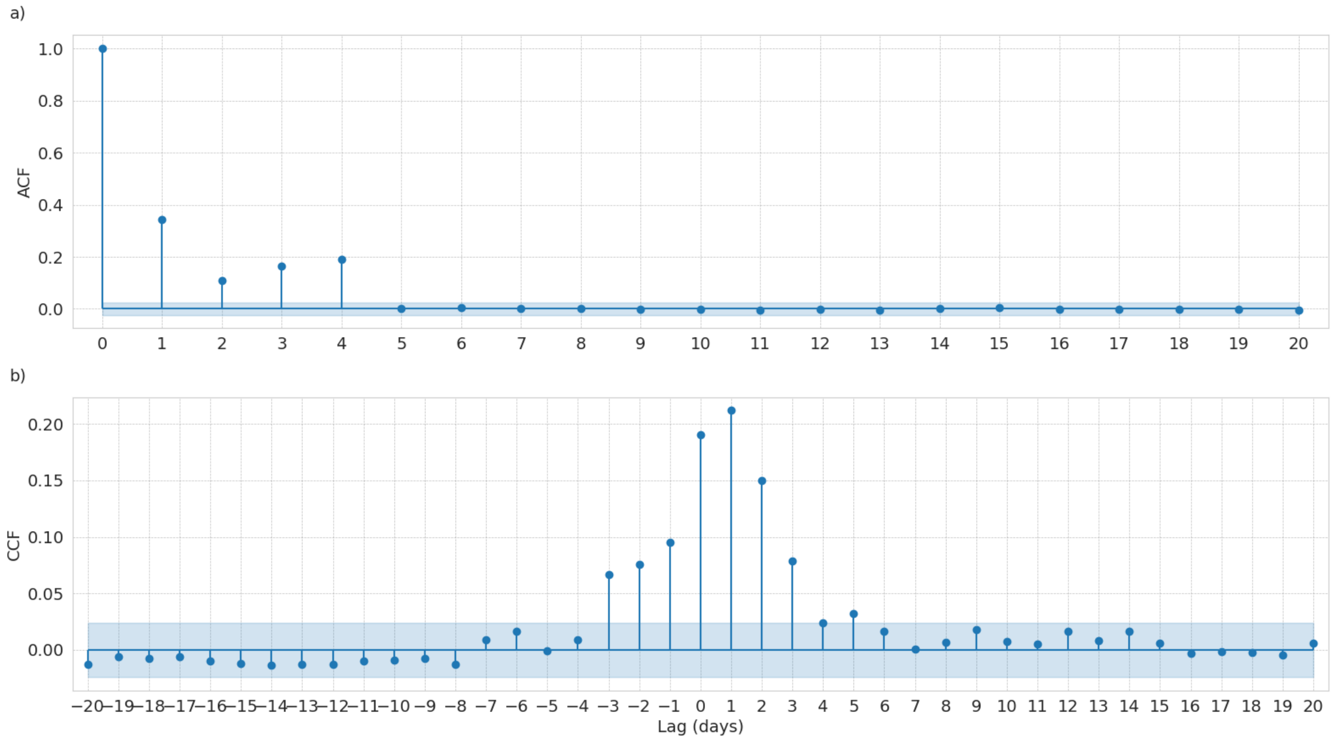

Figure S4: a) Autocorrelation of impact time series over 2003 to 2020; b) Cross-correlation of normalized and detrended time series of daily impact records and the local 99th percentile of daily precipitation fields from 2003 to 2020 based on SPARTACUS-TST. The shaded area represents the 0.05 significance threshold.

	areal mean				local p99				anomaly			
	SPARTACUS-TST	INCA	CERRA-Land	ERA5-Land	SPARTACUS-TST	INCA	CERRA-Land	ERA5-Land	SPARTACUS-TST	INCA	CERRA-Land	ERA5-Land
SPARTACUS-TST	-	87%	88%	84%	-	81%	78%	80%	-	81%	83%	75%
INCA	87%	-	82%	85%	82%	-	73%	75%	81%	-	73%	74%
CERRA-Land	88%	81%	-	78%	77%	73%	-	71%	83%	73%	-	72%
ERA5-Land	84%	85%	78%	-	81%	75%	71%	-	75%	74%	72%	-

Table S2: Portion of the 330 extreme events in common across datasets for each method. For each dataset in the left column, the number of event dates falling within any 5-day window of the events detected from every other dataset is counted.

	SPARTACUS-TST			INCA			CERRA-LAND			ERA5-Land		
	areal mean	local p99	anomaly	areal mean	local p99	anomaly	areal mean	local p99	anomaly	areal mean	local p99	anomaly
areal mean	-	84%	79%	-	79%	78%	-	88%	80%	-	83%	82%
local p99	84%	-	83%	79%	-	81%	88%	-	82%	82%	-	81%
anomaly	79%	83%	-	78%	81%	-	80%	82%	-	82%	81%	-

Table S3: Portion of the 330 extreme events in common across methods for each dataset. For each method in the left column, the number of event dates falling within any 5-day window of the events detected by every other method is counted.

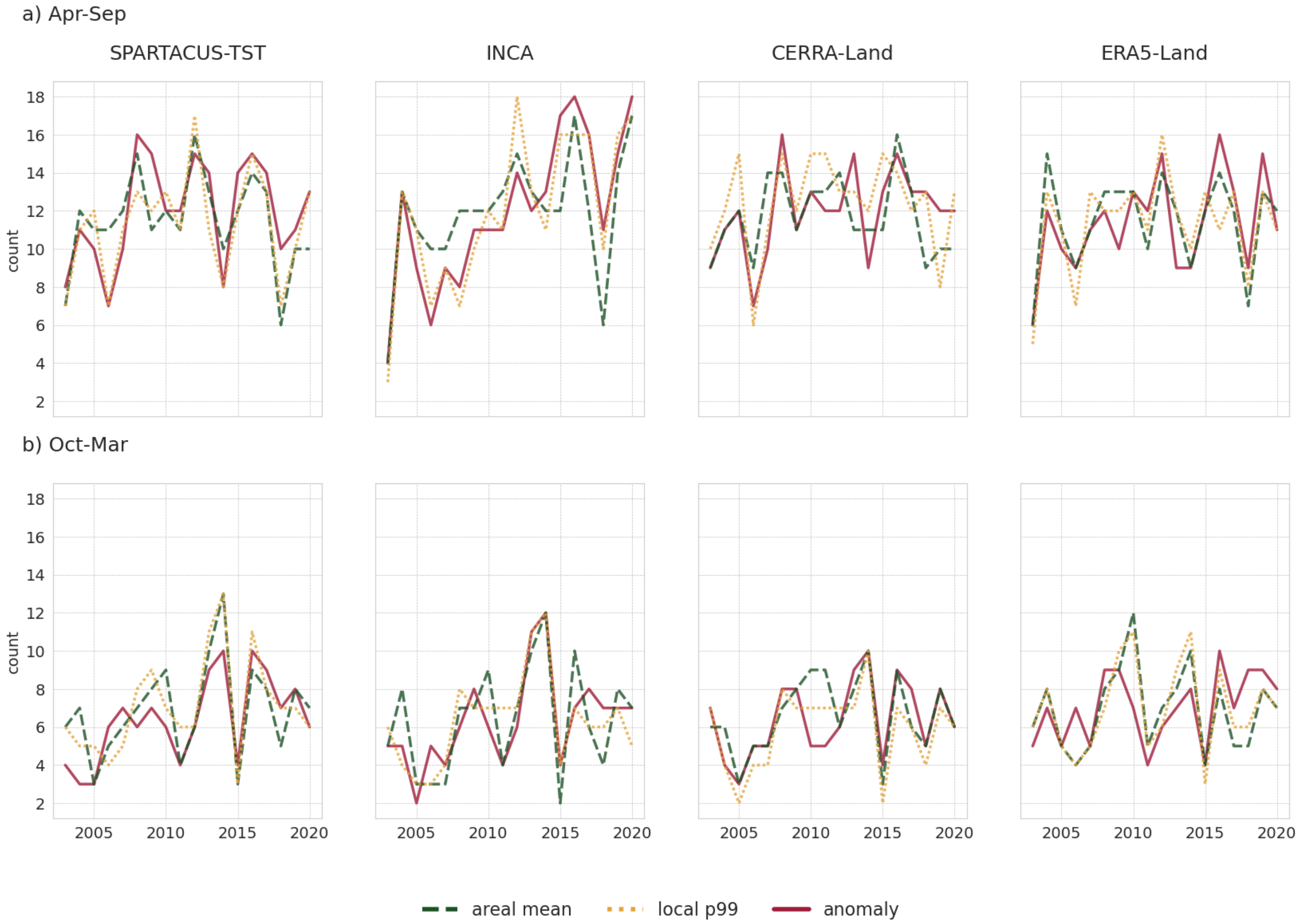

Figure S5: Event counts per year in a) summer half year (April to September) and b) winter half year (October to March) based on the top 5 % most extreme precipitation days detected by different methods from 2003-2020 for SPARTACUS-TST, INCA, CERRA-Land and ERA5-Land.

	areal mean	local p99	anomaly
SPARTACUS-TST	0.23	0.21	0.22
INCA	0.22	0.20	0.22
CERRA-Land	0.21	0.17	0.22
ERA5-Land	0.17	0.17	0.16

Table S4: Correlation coefficients of daily time series of impact records and different daily precipitation statistics used to detect extreme precipitation events over 2003-2020 for each dataset. The correlation is calculated for all years considering a lag of one day between precipitation statistics and impact counts.

FLOODS	**Areal mean**			**Local p99**			**Anomaly**		
	Year	**Summer**	**Winter**	**Year**	**Summer**	**Winter**	**Year**	**Summer**	**Winter**
SPARTACUS-TST	48.7	44.6	60.5	58.0	58.0	57.9	58.0	57.1	60.5
INCA	51.3	49.1	57.9	59.3	57.1	65.8	56.7	55.4	60.5
CERRA-Land	48.7	43.8	63.2	56.0	54.5	60.5	49.3	44.6	63.2
ERA5-Land	42.7	35.7	63.2	47.3	42.9	60.5	42.7	36.6	60.5

Table S5: Hit rate (%) as the portion of hazardous dates (i.e., dates with at least two flood records) occurring in coincidence of an extreme precipitation event (within a 5-day window centred on the extreme precipitation days) for each combination of datasets and methods and by considering the whole year, summer (April to September) and winter (October to March) half years. The top 5 % most extreme precipitation dates over 2003-2020 are considered (330 events).

MASS MOVEMENTS	Areal mean			Local p99			Anomaly		
	Year	Summer	Winter	Year	Summer	Winter	Year	Summer	Winter
SPARTACUS-TST	51.8	51.0	53.1	55.4	57.2	52.2	53.1	54.6	50.4
INCA	54.1	53.6	54.9	55.4	56.7	53.1	53.4	55.7	49.6
CERRA-Land	50.2	51.5	47.8	53.7	55.2	51.3	50.5	50.5	50.4
ERA5-Land	48.2	44.3	54.9	50.5	49.5	52.2	45.9	42.3	52.2

Table S6: Hit rate (%) as the portion of hazardous dates (i.e., dates with at least two mass movement records) occurring in coincidence of an extreme precipitation event (within a 5-day window centred on the extreme precipitation days) for each combination of datasets and methods and by considering the whole year, summer (April to September) and winter (October to March) half years. The top 5 % most extreme precipitation dates over 2003-2020 are considered (330 events).

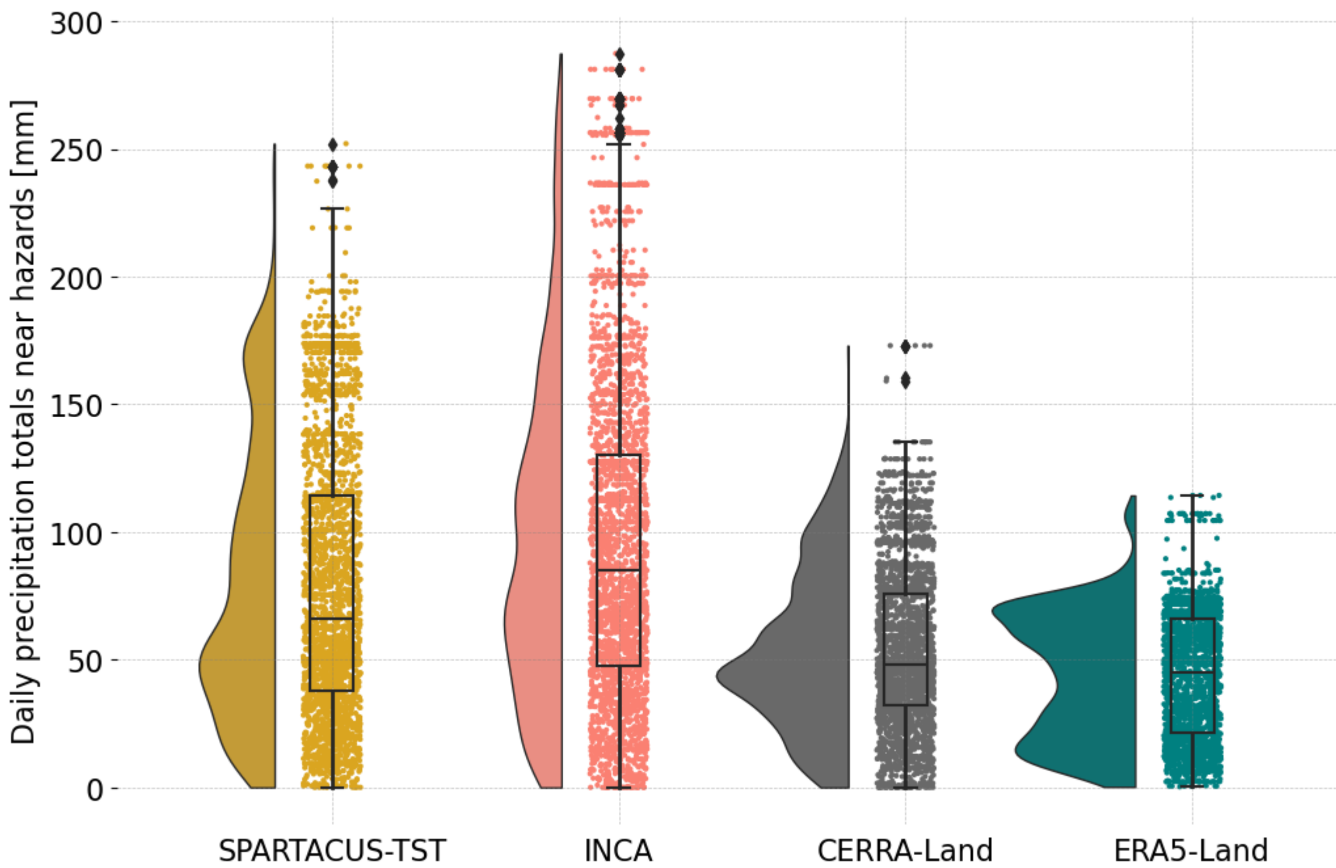

Figure S6: Distribution of 1-day precipitation intensities in the spatial proximity of recorded hazards for all datasets based on the most intense 5 % precipitation events (330 events) detected by the local p99 method. The precipitation intensities are extracted from the closest grid point to each hazard location without aggregating over co-occurring hazards.

dataset	method	mean [mm]	median [mm]	75^{th} percentile [mm]	max [mm]	absolute max [mm]
SPARTACUS-TST	local p99	46.0	41.5	60.2	180.9	252.1
	areal mean	45.2	38.8	60.2	180.9	252.1
	anomaly	45.7	41.4	60.2	180.9	252.1
INCA	local p99	53.4	45.8	74.2	202.5	287.4
	areal mean	51.9	45.0	72.1	202.5	287.4
	anomaly	52.6	45.3	71.9	202.5	287.4
CERRA-Land	local p99	37.7	36.5	48.5	116.6	173.0
	areal mean	39.9	37.1	48.5	142.4	173.0
	anomaly	39.1	37.0	49.5	142.4	173.0
ERA5-Land	local p99	25.8	22.2	32.5	83.8	114.3
	areal mean	27.0	23.4	32.8	83.5	98.8
	anomaly	27.0	23.4	33.4	83.5	98.8

Table S7: Summary statistics for median daily precipitation intensity in the proximity of hazard records (2003-2020) based on the 330 precipitation events detected by each dataset-method combination. Statistics is calculated over precipitation intensities extracted from the closest grid point to each impact location for which the median values over all hazard records on the same date are considered. In the last column the absolute maxima of local intensities without calculating the median are reported.

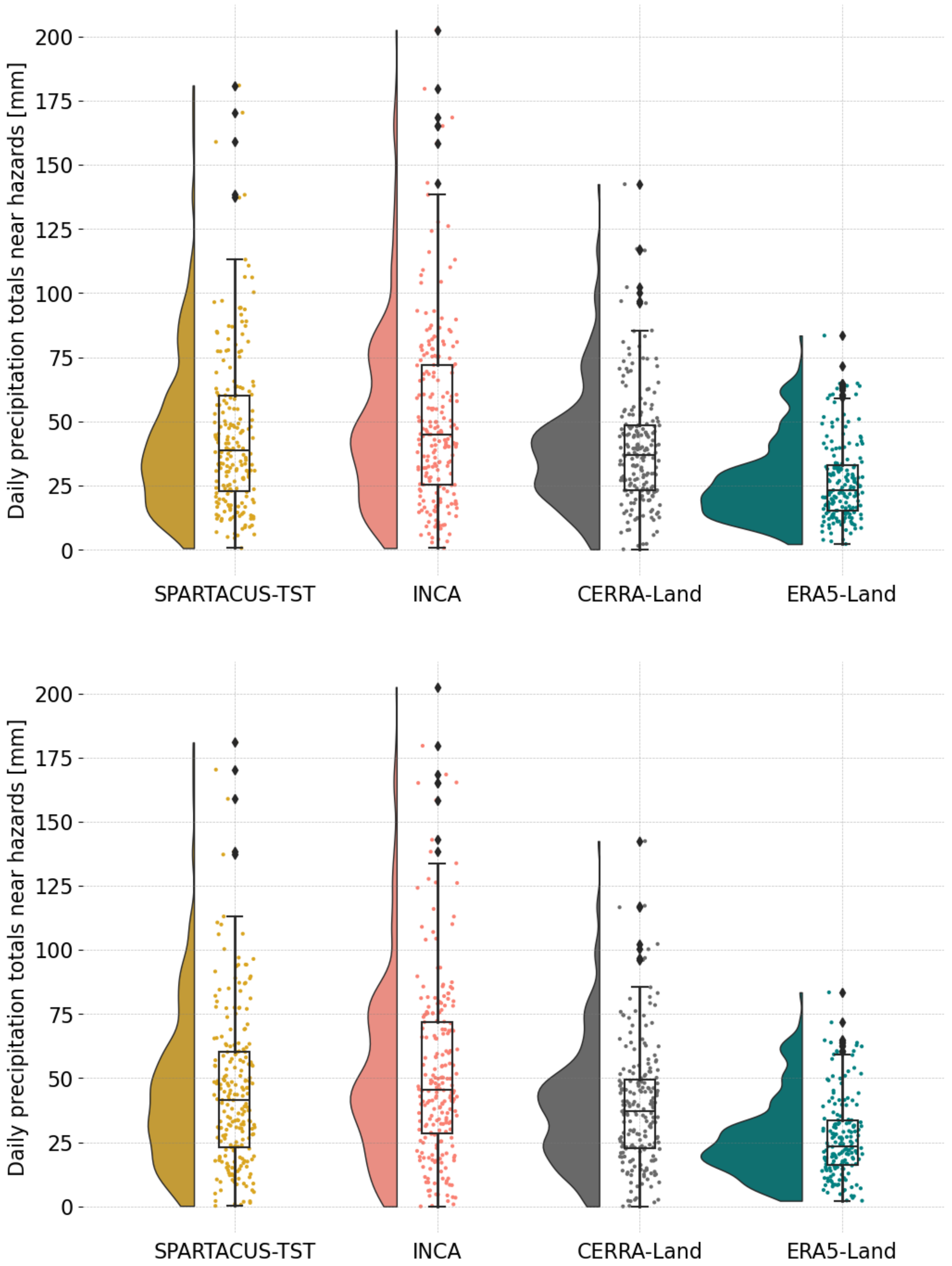

Figure S7: Distribution of 1-day precipitation intensities in the spatial proximity of recorded hazards for all datasets based on the most intense 5 % precipitation events (330 events) detected by the areal mean (upper panel) and the anomaly method (lower panel). The precipitation intensities are extracted from the closest grid point to each hazard location and the median values over all hazard records on the same date are displayed.

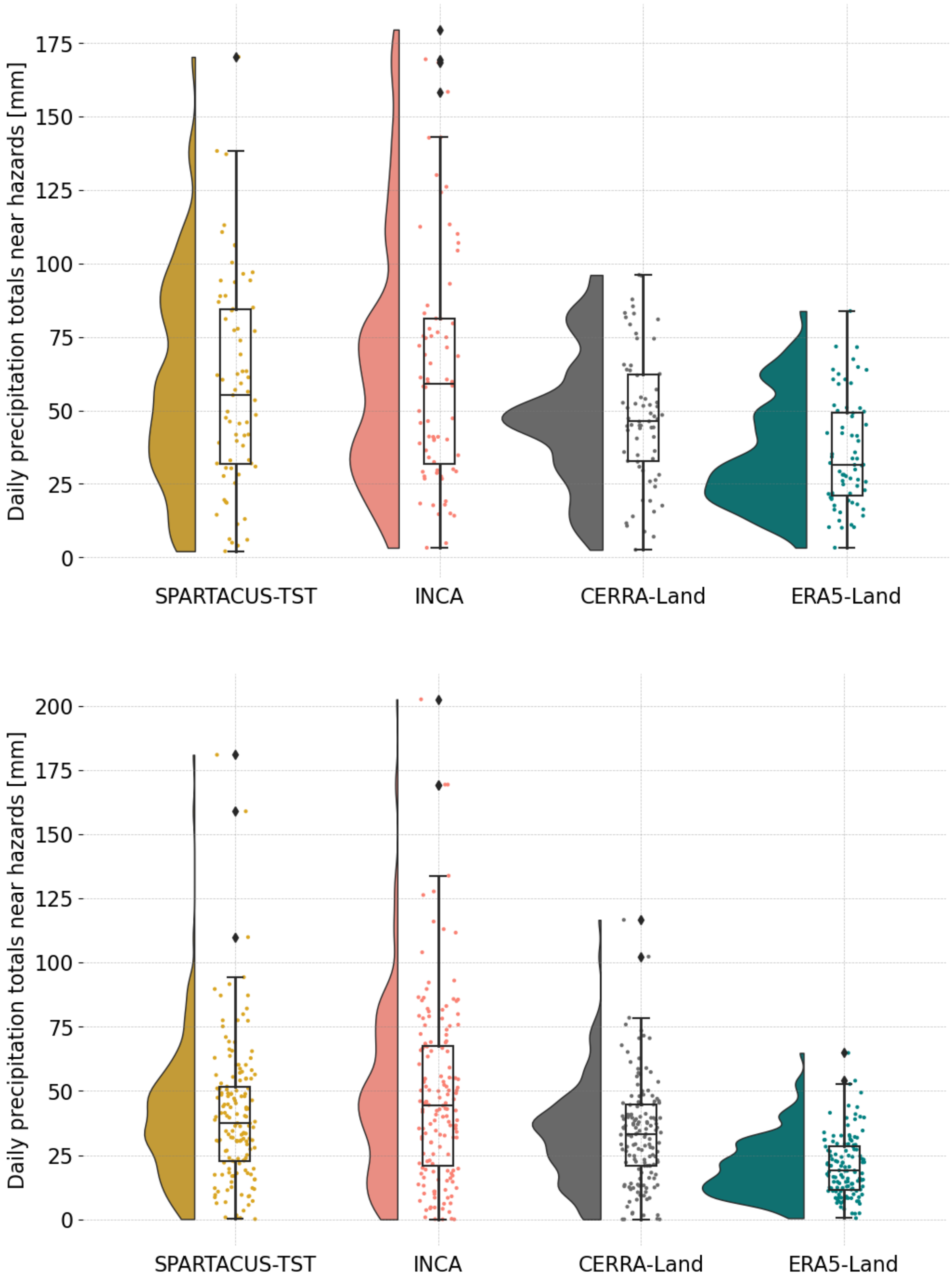

Figure S8: Distribution of precipitation intensities in the spatial proximity of recorded hazards for all datasets for the winter half year (October to March; upper panel) and the summer half year (April to September; lower panel) detected by the local p99 method. The precipitation intensities are extracted from the closest grid point to each hazard location and the median values over all hazard records on the same date are displayed.